Available online at www.sciencedirect.com
SCIENCE DIRECT®
Journal of Nuclear Materials 353 (2006) 12–18
journal of nuclear materials
www.elsevier.com/locate/jnucmat

The microstructural modelling of nuclear grade graphite

G. Hall *, B.J. Marsden, S.L. Fok

Nuclear Graphite Research Group, School of Mechanical, Aerospace and Civil Engineering, The University of Manchester, P.O. Box 88, Manchester M60 1QD, United Kingdom

Received 26 August 2005; accepted 1 February 2006

Abstract

By using the finite element method it has been possible to simulate irradiation-induced property changes, namely dimensional and Young's modulus changes, from which the probable microstructural mechanisms have been identified. In the finite element models, both property changes were shown to be dependent upon the filler particle dimensional changes and the accommodation porosity. However, these need to be corroborated through the examination of actual specimens. Further work is also required to adapt the procedure to other graphites, reactor conditions, and material properties.

1. Introduction

When graphite is used in a nuclear reactor it will experience significant property changes as a result of temperature variations, fast neutron irradiation, and in CO_2-cooled and air-cooled reactors, radiolytic oxidation. Experimental observations from material test reactors (MTRs) have shown these changes to be highly complex, although numerous authors [1–9] have proposed various mechanisms and relationships for the changes. Some have focused upon individual properties whilst others have examined the inter-relationship between two properties, but these usually provide little or no insight into what microstructural mechanisms are causing the observed property changes.

Initial studies [10] in using the finite element method to model graphite microstructure and property changes showed promising results. These have been developed further to an extent where the probable microstructural mechanisms behind irradiation-induced dimensional and Young's modulus changes can be proposed.

2. Nuclear grade graphite

Graphite used in nuclear reactors, or more specifically that used as a moderator, is manufactured utilising the production techniques of graphite electrodes, with special attention given to the removal of impurities. The main constituent is the filler, generally a petroleum or natural based coke. A binder, such as coal-tar pitch, is mixed with the blended filler particles and formed into the required shape using extrusion or pressing. This is then baked at ≈1000 °C (calcination) and impregnated with pitch

* Corresponding author. Tel.: +44 161 275 4391; fax: +44 161 275 4328.
E-mail address: graham.n.hall@manchester.ac.uk (G. Hall).

0022-3115/$ - see front matter © 2006 Elsevier B.V. All rights reserved.
doi:10.1016/j.jnucmat.2006.02.082

to increase its density. Further heating to ≈2800 °C graphitises the material, and after cooling, it will be machined to its required dimensions.

Numerous graphites have been developed worldwide, with some having anisotropic material properties and others being near-isotropic. The directional dependence can be a result of the filler used, the manufacturing process, or a combination of both. This can be demonstrated by two graphites used in the UK: Pile grade A and Gilsocarbon.

Pile grade A (PGA) was manufactured for use in the early gas-cooled reactors and used filler particles derived from the petroleum industry [11]. These particles tended to have an elongated, needle-like shape that would preferentially align with the extrusion axis (Fig. 1(a)). As the crystallites within the filler particle were also preferentially aligned, the bulk material had anisotropic material properties. Gilsocarbon was a later classification of graphite developed for the advanced gas-cooled reactors (AGRs) [11]. The filler was this time obtained from a naturally occurring asphalt mined in the USA called Gilsonite. The coke manufactured from Gilsonite produced spherical, onion-like filler particles that had no preferential alignment to the manufacturing process (Fig. 1(b)). As the crystallites within the particles tended to align circumferentially, the bulk material has near-isotropic behaviour.

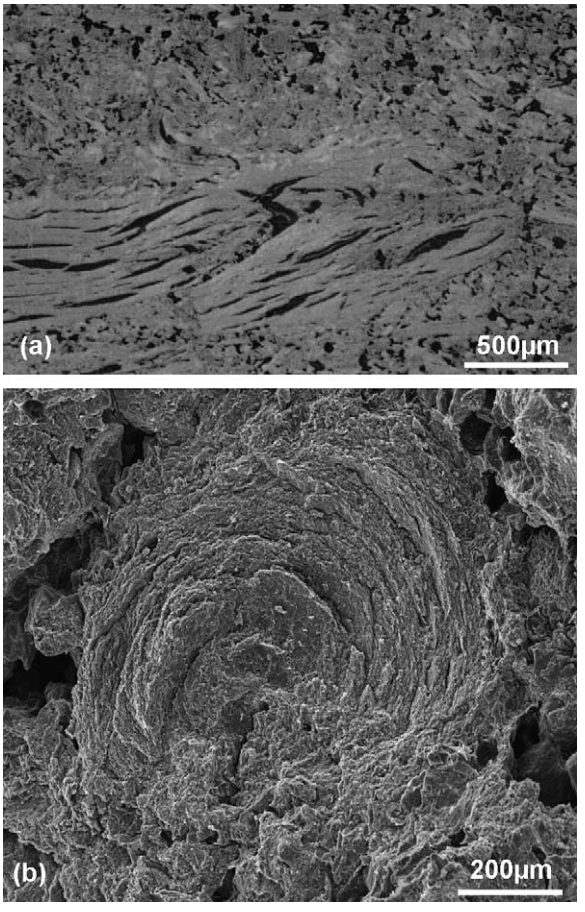

Fig. 1. Nuclear grade graphite: (a) PGA (courtesy of G. Neighbour) and (b) Gilsocarbon (courtesy of S. Fazluddin).

In both types of graphite, the binder and impregnant crystallites are randomly oriented and do not have any preferential alignment. Within the structure there are also different scales of porosity ranging from large gas-evolution pores, calcination cracks, and microporosity formed during cooling from graphitisation temperatures often referred to as Mrozowski cracks [12].

The complexity of the irradiation-induced property changes can be exemplified by the dimensional change behaviour of Gilsocarbon (Fig. 2). At irradiation temperatures of ≈430 °C, the graphite expands at very low doses, but as the fast neutron dose increases, the graphite contracts. As the dose increases further, the shrinkage rate reduces and the graphite begins to expand; this reversal in shrinkage is known as turnaround. If the irradiation temperature is increased (≈600 °C), the rate at which the graphite contracts increases, as does the rate of expansion after turnaround. The dose at which turnaround occurs also reduces. Increasing the irradiation temperature even further (≈940 °C) does not significantly alter the rate of shrinkage, but the dose at which turnaround occurs is lower and the rate of expansion afterwards is higher. Above irradiation temperatures of ≈1000 °C, there appears to be no initial expansion or slow rate of shrinkage, with the remaining shrinkage being at a higher rate than the shrinkage at lower irradiation temperatures. Again, as the temperature increases, the dose at which turnaround occurs reduces, and

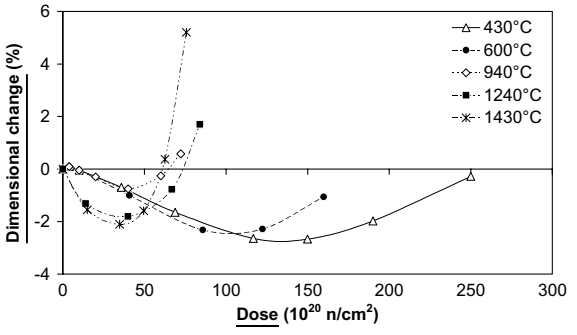

Fig. 2. Gilsocarbon dimensional changes.

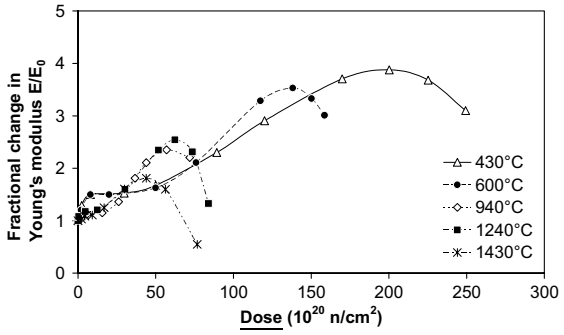

Fig. 3. Gilsocarbon Young's modulus.

the subsequent growth is at a faster rate. However, the amount of shrinkage before turnaround increases with increasing irradiation temperature.

The Young's modulus changes are of similar complexity (Fig. 3). At ≈430 °C and low doses, the Young's modulus increases rapidly, and then remains approximately constant. Increasing the dose causes a second increase to a greater magnitude but at a slower rate. Eventually, as the irradiation continues, the rate of increase diminishes and the Young's modulus reduces. Increasing the irradiation temperature to ≈600 °C increases the rates of the second increase and of the decrease, but the maximum Young's modulus will be less. Raising the temperature to ≈940 °C has a similar effect but the initial increase and the decrease rate reduce. At even higher temperatures (>1200 °C) the rate of the second increase and of the decrease reduce with increasing temperature. The magnitudes also reduce but at ≈1200 °C, the maximum Young's modulus is greater than that at ≈940 °C. The dose at which the Young's modulus decreases also reduces with increasing temperature.

Various authors have postulated what mechanisms cause the observed changes, such as growth of crystallites, formation and closure of porosity, and pinning and tightening of the graphite structure. It was upon these hypotheses that this work was based.

3. Finite element modelling

The underlying assumption of this procedure was that the filler behaviour was the dominant force behind the polycrystalline material changes. Therefore, the first stage was to create an idealised filler particle. Using Gilsocarbon as an example, the spherical filler particle was not explicitly represented, but instead a needle-shaped filler particle was created (Fig. 4); the isotropy would be accounted for in the polycrystalline stage. The dimensions of the filler particle were based upon the study by White [13] and the lenticular cracks (accommodation porosity) on that by Sutton and Howard [4]. A layer of material representing binder, surrounded the filler particle in order to provide a restraining effect. Numerous filler models were analysed with different dimensions, material ratios (filler to binder), and accommodation porosity percentages, in order to provide a range of filler particle behaviours.

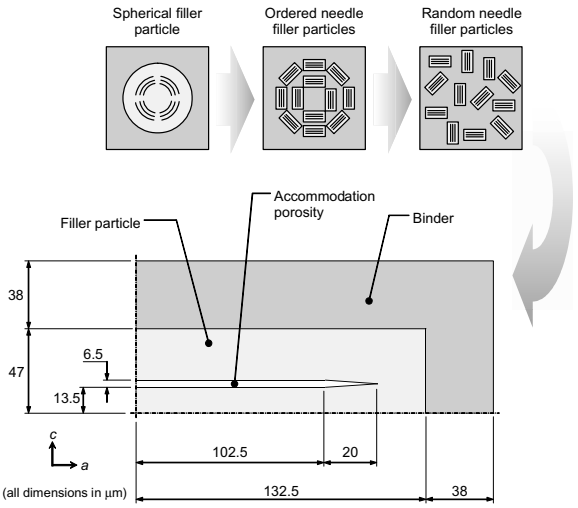

Fig. 4. Finite element filler model (dimensions adapted from Refs. [4] and [13]).

As the underlying assumption was that the filler behaviour was dominant, the filler particle was assigned irradiation dependent properties of highly annealed pyrolytic graphite (HAPG) [14–18], but the binder was assigned unirradiated properties of an isotropic graphite (Gilsocarbon) [3] as it was only included to act as a restraint. The model was then subjected to loading conditions representative of those found in a thermal reactor, and the apparent behaviour obtained (Fig. 5). This behaviour was then used in the next modelling stage, a polycrystalline model (Fig. 6). It should be noted that due to the limited dose range of HAPG data, the filler particle and polycrystalline models were only analysed to 160×10^{20} n/cm^2. The HAPG data would have to be extrapolated to analyse the model at higher doses.

In the polycrystalline model, elements could be assigned filler particle properties obtained from the

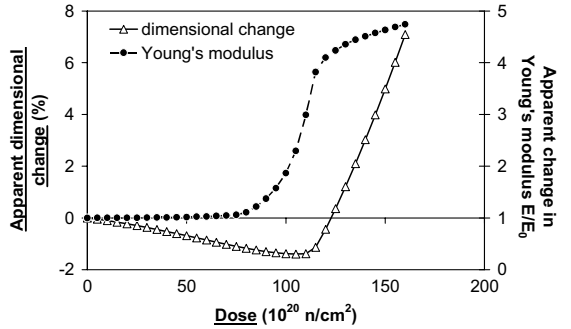

Fig. 5. Example filler model apparent behaviour (*c*-axis).

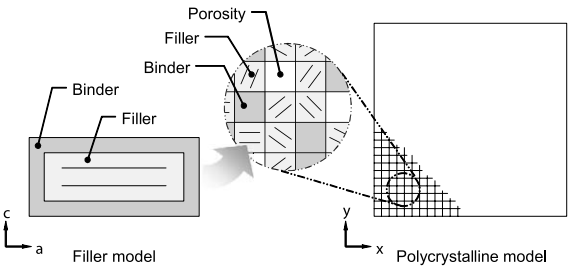

Fig. 6. Polycrystalline finite element model.

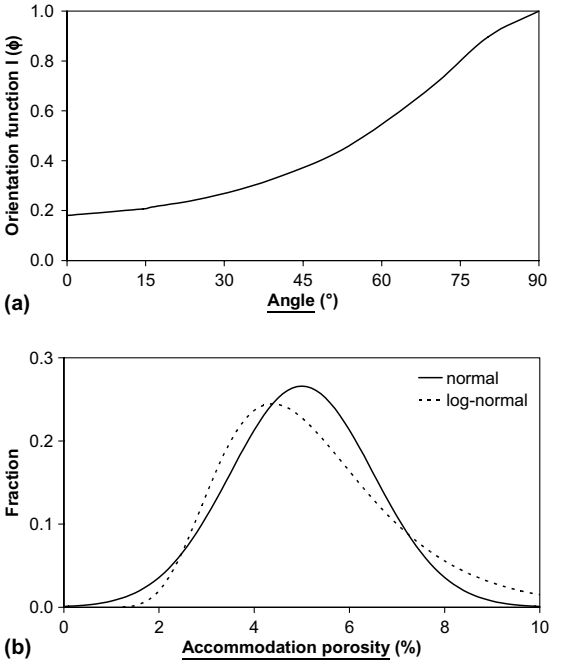

Fig. 7. Polycrystalline model distributions: (a) filler orientations for an anisotropic graphite and (b) accommodation porosity distribution.

previous modelling stage, binder properties, or negligible properties (unirradiated properties of low magnitudes to symbolise porosity). The assignment of elements was randomly distributed throughout the model and the filler particle elements could be oriented to give the required material; for an isotropic material there was an even distribution of orientations, while the anisotropic material would have a preferential alignment [4] (Fig. 7(a)). Different filler particle behaviour could be assigned to the elements to account for a distribution of crack sizes [19,20] (Fig. 7(b)), and the percentages of porosity and binder could be modified according to the specific graphite composition [21]. The polycrystalline model was then loaded as per the filler model and the apparent behaviour compared with experimental behaviour.

4. Results

Comparison of the finite element dimensional changes with experimental data showed similarities in trends and magnitudes, especially at the lower temperatures (Fig. 8). At 450 °C, the finite element dimensional changes contracted slowly at very low doses, and then at an accelerated rate as the dose

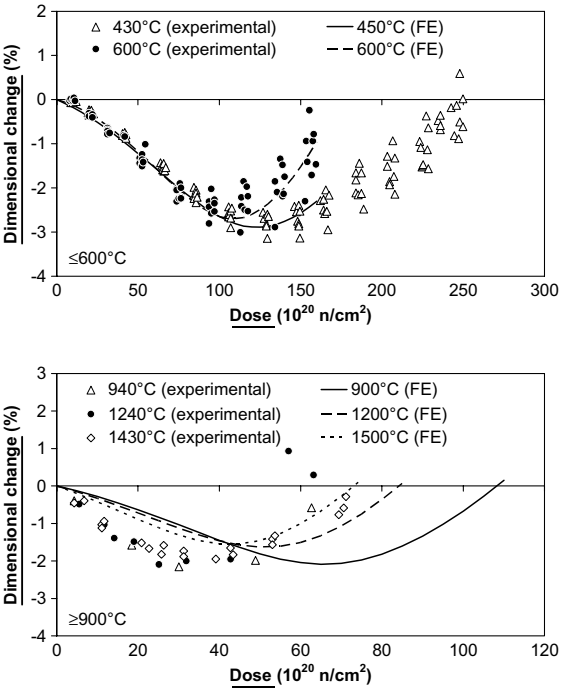

Fig. 8. Apparent and experimental dimensional changes of an isotropic graphite.

increased. As the irradiation continued, turnaround was exhibited and the model began to expand. These changes all occurred within the scatter of the data. At 600 °C, the behaviour was similar except that the initial shrinkage was at a lower rate, the main shrinkage was at a faster rate, turnaround occurred at a lower dose and magnitude, and the subsequent expansion was at a higher rate. These changes were also within the scatter of the data. At temperatures above 600 °C, the initial contraction was at a higher rate, similar to that of the main shrinkage, with the higher the temperature, the quicker the shrinkage rate, although the rates at 1200 and 1500 °C were the same. The dose and magnitude at turnaround were lower, and reduced as the temperature increased. The rate of expansion after turn around was higher and increased as the temperature increased; again the rates at 1200 and 1500 °C were the same.

The finite element and experimental Young's modulus changes also exhibited some similarities, with the lower temperatures again being closer to experimental data (Fig. 9), although these were not as close as the equivalent dimensional changes. It must be noted that the initial increase in Young's modulus is understood to be a consequence of mechanisms at the atomic scale [22], and thus was not examined here. At 450 °C, the Young's modulus was constant at lower doses, but as the dose increased, the modulus increased. The trend was the similar to the experimental data but the magnitudes were noticeably smaller in the finite element predictions. The changes at 600 °C were comparable but the rates of change were higher; again the magnitudes were smaller than the experimental changes at this temperature. Increasing the temperature further caused the increases to occur at lower doses and at higher rates. At all temperatures there was no reduction in Young's modulus at the higher doses, instead there was a steady increase.

When the binder Young's modulus was allowed to reduce with stress (450 and 600 °C finite element models only), a reduction in the Young's modulus at high doses could be seen (Fig. 10). Examination of the dimensional changes at these temperatures showed that the dimensional change rates had not significantly changed (Fig. 11).

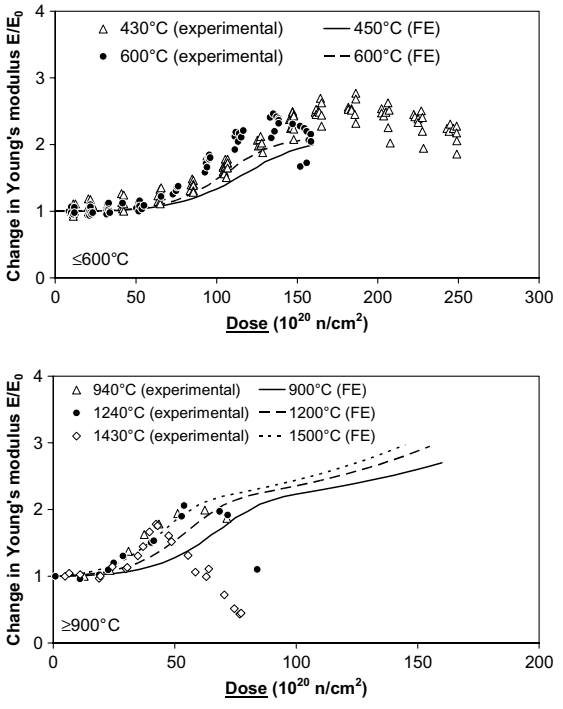

Fig. 9. Apparent and experimental Young's modulus changes of an isotropic graphite.

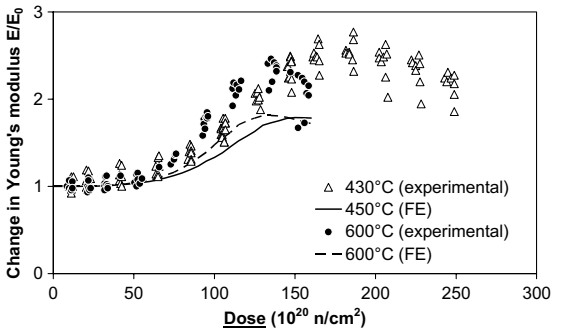

Fig. 10. Apparent and experimental Young's modulus changes of an isotropic graphite (binder Young's modulus stress dependent).

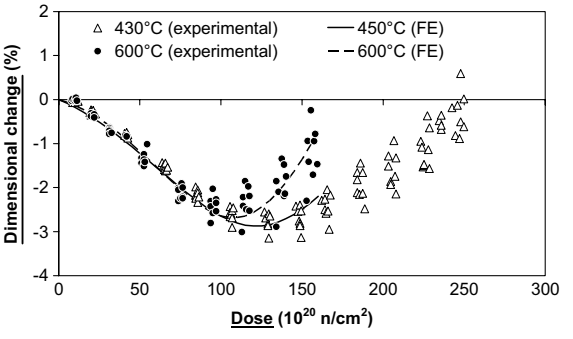

Fig. 11. Apparent and experimental dimensional changes of an isotropic graphite (binder Young's modulus stress dependent).

5. Discussion

At 450 °C, the dimensional changes of the finite element demonstrated two rates of shrinkage, low at low doses and higher as the dose increased. The shrinkage occurred because the accommodation allowed the filler *a*-axis contraction to dominate as the *c*-axis expansion was absorbed by the accommodation porosity. The initial slow rate of shrinkage can be attributed partly to the lower rate of dimensional change rates of HAPG at these lower doses, and to the initial closure of small quantities of accommodation porosity. The increase in shrinkage rate corresponded to the increase in HAPG dimensional change rate and further closing of the accommodation porosity. When the majority of the accommodation porosity was fully closed, the material began to expand as the *c*-axis expansion became dominant. The smooth transition between the shrinkage and expansion was a consequence of the distribution of accommodation porosity within the polycrystalline model.

The finite element results at 600 °C were initially similar to those at 450 °C because the dimensional changes of the HAPG at this temperature were similar to those at 450 °C. Turn around occurred at a lower dose because more of the accommodation porosity had been taken up by thermal expansion and the dimensional change rate of HAPG was slightly higher at this dose when compared to that at 450 °C. The latter also caused the higher rate of expansion after turn around.

At the higher temperatures ($\geqslant$600 °C), the finite element dimensional changes demonstrated an increasing rate as the HAPG dimensional changes were higher at these temperatures. There was less noticeable, if any, slow shrinkage at the low doses as although the HAPG dimensional changes still had a slower rate of change at these doses, the initial accommodation had been absorbed by the thermal expansion. The dimensional changes at 900 °C were significantly different from the experimental data because of the HAPG dimensional change data used. Three dimensional change temperature curves (430, 600 and 1250 °C) were used for the filler particle models, and when the temperature was set to 900 °C, the finite element program linearly interpolated between the two closest temperatures (600 and 1250 °C). However, the experimental data implies that there is a significant change in behaviour above 900 °C. Therefore, it may have been more realistic to have had a 900 °C dimensional change curve close to those at 430 and 600 °C. Unfortunately, experimental data for such a curve were not available.

The Young's modulus changes at the lower temperatures exhibited trends comparable to the experimental data. At 450 °C and low doses, the Young's modulus was approximately constant as the majority of the accommodation porosity was still open. The increase in Young's modulus as the dose increased occurred when more of the accommodation porosity began to close. The shape of the increase (slow, fast and then slow again) can be attributed to the normal distribution of the accommodation porosity within the polycrystalline model. The shift in the Young's modulus curve to the left as the temperature increased was a result of the thermal expansion partially or fully closing some of the accommodation porosity. Thus, the dimensional changes closed the remaining accommodation porosity at a lower dose. The increase in rate as the temperature increased was because of the increase in HAPG dimensional change rate with increasing temperature. Similarly, the difference between experimental and finite element results at these higher temperatures was a result of the lack of HAPG dimensional change curves at sufficient irradiation temperatures, as stated for the dimensional change results. The increase in Young's modulus at higher doses in the higher-temperature models was contrary to experimental observations. This was assumed to be caused by the increase in internal stress within the models as no form of cracking was included.

Microstructural cracking has been shown to occur at the filler/binder interface [23] and therefore, allowing the Young's modulus of the binder to decrease when a stress limit was reached was assumed to be a simplified method of modelling this process. As the model reached a dose where the majority of the accommodation porosity was fully closed, the stress increased to a level higher than the defined stress limit. Consequently, the binder Young's modulus reduced and the bulk Young's modulus reduced. As the stress increased with increasing dose, more binder 'cracked' and the Young's modulus continued to reduce. This reduction did not adversely effect the dimensional changes as the main driving force behind these changes was the filler particles and not the binder. The only noticeable effect was that the dimensional change rate increased as the decrease in binder Young's modulus reduced the restraining effect upon the filler particles.

If these models were, as assumed here, an acceptable representation of the real graphite microstructure, the finite element model changes should have a real microstructure equivalent. The dominant factors in the finite element dimensional and Young's modulus changes were the filler particle dimensional changes and the accommodation porosity. The filler particle dimensional changes can be directly related to its real counterpart, but the accommodation porosity requires further substantiation. The closure of such porosity has been shown in the finite element models to cause turnaround and increases in Young's modulus, but it is not known which porosity this relates to in the real structure and whether it can be seen to close in a comparable manner. Examination of irradiated samples would help to identify which porosity types (calcination cracks, Mrozowski type cracks, or both) are of interest.

The mechanisms identified using the finite element models should be applicable to any graphite as they all comprise of the same basic constituents, the differences arise from the specific arrangement and composition of the graphite. Therefore, it should be possible to apply this technique to other graphites such as PGA (this has been done to some degree), IG110 etc. Similarly, different operating conditions including lower and higher temperatures, and radiolytic oxidation require investigation.

6. Conclusions

Idealised finite element models of graphite filler particle and polycrystalline structures were created. The main assumption was that the filler particle behaviour is the driving force behind the polycrystalline changes. The models were assigned experimentally obtained material properties for the equivalent graphitic material, with the composition and arrangement of these materials being based upon experimental and manufacturing data.

The models demonstrated that the closure of accommodation porosity caused dimensional change turnaround and the increase in Young's modulus in the polycrystalline material. The polycrystalline dimensional and Young's modulus change rates increased with temperature as a result of the increase in crystallite dimensional change rates with higher temperatures. At higher temperatures, the closure of the smaller accommodation porosity in the polycrystalline graphite by thermal expansion caused the initial shrinkage and the dose at which the Young's modulus increased to change. The reduction in polycrystalline Young's modulus at high doses was due to microcracking, possibly at the filler/binder interface. However, irradiated samples need to be inspected to substantiation these mechanisms, particularly accommodation porosity closure.

Acknowledgements

The financial support of British Energy plc. and the IMC is gratefully acknowledged. The views expressed in this paper are those of the authors and do not necessarily represent the views of the sponsors.

References

[1] J.H.W. Simmons, Radiation Damage in Graphite, Pergamon, 1965.
[2] B.T. Kelly, Proposals for a revised method of calculating the thermal expansion of graphites and fuel compacts, UK Public Records Office, AB 7/21684, 1971.
[3] J.E. Brocklehurst, B.T. Kelly, Carbon 31 (1993) 155.
[4] A.L. Sutton, V.C. Howard, J. Nucl. Mater. 7 (1963) 58.
[5] G.M. Jenkins, J. Nucl. Mater. 13 (1963) 33.
[6] W.C. Morgan, Carbon 4 (1966) 215.
[7] G.B. Neighbour, J. Phys. D: Appl. Phys. 33 (2000) 2966.
[8] G. Hall, B.J. Marsden, S.L. Fok, J. Smart, Nucl. Eng. Des. 222 (2003) 319.
[9] P.J. Hacker, G.B. Neighbour, B. McEnaney, J. Phys. D: Appl. Phys. 33 (2000) 991.
[10] G. Hall, Finite element analysis of crystals, University of Manchester, BEng undergraduate project, 1999.
[11] B.T. Kelly, The Structure and manufacture of nuclear grade graphite, Irradiation damage in graphite due to fast neutrons in fission and fusion systems, IAEA-TECDOC-1154, IAEA, 2000.
[12] S. Mrozowski, Mechanical strength, thermal expansion and structure of cokes and carbons, in: Proceedings of the 1st and 2nd Conferences on Carbon, 1956, p. 31.
[13] E.S. White, Some factors affecting the anisotropy of extruded carbon, in: Proceedings of the Fourth Carbon Conferences, University of Buffalo, Buffalo, New York, 1960, p. 681.
[14] J.E. Brocklehurst, B.T. Kelly, Carbon 31 (1993) 179.
[15] J.C. Bokros, G.L. Guthrie, D.W. Stevens, Carbon 9 (1971) 349.
[16] B.T. Kelly, Carbon 13 (1975) 350.
[17] A.C. Bailey, B. Yates, J. Appl. Phys. 41 (1970) 5088.
[18] O.L. Blakslee, D.G. Proctor, E.J. Seldin, G.B. Spence, T. Weng, J. Appl. Phys. 41 (1970) 3373.
[19] S. She, J.D. Landes, Int. J. Fracture 63 (1993) 189.
[20] M. Saichi, H. Shinohe, H. Mihashi, Trans. Jpn. Concr. Inst. 23 (2002) 25.
[21] R.E. Nightingale (Ed.), Nuclear Graphite, Academic Press, 1962.
[22] J.H.W. Simmons, The effects of irradiation on the mechanical properties of graphite, in: Proceedings of the Third Conference on Carbon, 1957, p. 559.
[23] Y.I. Shtrombakh, B.A. Gurovich, P.A. Platanov, V.M. Alekseev, J. Nucl. Mater. 225 (1995) 273.